Bulletin of the Seismological Society of America, Vol. 103, No. 6, pp. 3104–3114, December 2013, doi: 10.1785/0120130042

Precursory Seismic Activity Surrounding the High-Slip Patches of the 2011 M_w 9.0 Tohoku-Oki Earthquake

by Tamao Sato, Shinya Hiratsuka,* and Jim Mori

Abstract Using the Japan Meteorological Agency earthquake catalog since 1923, we investigated the seismic activity prior to the 2011 M_w 9.0 Tohoku-Oki earthquake with reference to the slip distribution, which is characterized by two high-slip ($\geq$20 m) patches separated by a zone of relatively low slip. The peak of the northern high-slip patch is located near the trench while the peak of the southern high-slip patch is situated about 40 km southeast of the mainshock epicenter, about 70 km away from the trench. It is estimated that the mainshock ruptured the southern high-slip patch first and then extended to a larger adjacent region, including the northern high-slip patch. The epicenters of foreshock activity that started two days before the mainshock are distributed in the western edge of the northern high-slip patch where other prominent activity, such as the 1981 event, occurred during the past 90 years. Based on the spatiotemporal seismicity pattern around the two high-slip patches, we infer that the foreshock activity triggered the 2011 Tohoku-Oki earthquake because the increased stress from the foreshock activity was able to overcome the strength of the southern high-slip patch, which had been sufficiently weakened by a series of large surrounding earthquakes since 2003. Other prominent activity, such as the 1981 event, failed to trigger such a great earthquake because similar stress condition had not been established at those times. The doughnut-shaped seismicity pattern that formed around the peak of the southern high-slip patch suggests the existence of an extremely strong patch that had not been ruptured by the surrounding large earthquakes for a long period of time.

Introduction

The 11 March 2011 Tohoku-Oki earthquake (M_w 9.0) occurred on the megathrust along the western margin of the Pacific Ocean where the Pacific plate is being subducted beneath the island of Honshu, Japan. The slip near the Japan Trench was estimated to be enormous; it averaged about 40 m over the upper 100 km of the megathrust and peaked at 60–80 m close to the trench (Lay *et al.*, 2011; Iinuma *et al.*, 2012; Ozawa *et al.*, 2012). Nearly a thousand years are required to accumulate such a large slip for the convergence rate of 8–9 cm/yr along this plate boundary zone. In recent years, a dominant group of earthquakes in the hypocentral area of the 2011 earthquake consisted of M 7 interplate events that occurred in the deep portion of the megathrust. This led to a high probability estimate of an M 7 earthquake in the near future off the coast of Miyagi prefecture (Earthquake Research Committee [ERC], 2009). Although a strong plate coupling was estimated from the crustal deformation observed by the Global Positioning System (GPS) stations for the deep portion of the megathrust off the coast of the Miyagi prefecture, the shallow portion of the megathrust was not thought to be accumulating a large slip deficit (e.g., Suwa *et al.*, 2006).

Two days before the Tohoku-Oki earthquake, foreshock activity (largest event M 7.3) occurred north of the mainshock epicenter. The epicentral area of the foreshock activity is similar to an M 7.0 earthquake in 1981 (Shao, Ji, and Zhao, 2011). The question arises, "Why did the 1981 event not trigger a great earthquake"? A time difference of 30 years is negligible in comparison with the long time required for the slip deficit of more than 40 m. In order to address this question, we investigate the past seismicity in the hypocentral area of the 2011 Tohoku-Oki earthquake with reference to its slip distribution. We use the earthquake catalog compiled by the Japan Meteorological Agency (JMA) since 1923. The hypocenter parameters in the catalog are those determined using the arrival times of seismic phases recorded on seismograms, thus providing reliable information on the seismicity in Japan for the past 90 years. The earthquake catalog indicates that other prominent activity other than the 1981 event also occurred in the same epicentral area in the past. We explore the reasons why a great earthquake like the 2011

*Now at Institute of Seismology and Volcanology, Hokkaido University, Sapporo 060-0810, Japan.

Tohoku-Oki earthquake was not triggered by those events. We assume the variations of stress accumulation on the megathrust, as suggested by the complex slip distribution of the Tohoku-Oki earthquake, would manifest itself in the spatiotemporal distribution of seismic activity. Because the interpretation of the seismicity pattern depends on the mainshock slip distribution, it is necessary to have a reliable model.

Twin-Peaks Slip Distribution

A number of fault models for the Tohoku-Oki earthquake have already been determined using the seismic, geodetic, and tsunami data (e.g., Fujii *et al.*, 2011; Ide *et al.*, 2011; Ozawa *et al.*, 2011). For the purpose of the present study, however, we independently determine the slip distribution based on a fault geometry that matches the configuration of the upper interface of the subducted Pacific plate obtained by Takeuchi *et al.* (2008). Previously, we determined the slip distribution of the 2011 Tohoku-Oki earthquake adopting the same fault geometry (Sato *et al.*, 2012). At that time, we used only the coseismic displacements derived from the GEONET GPS stations on land (Ozawa *et al.*, 2011). In addition to that dataset, here we also use the coseismic displacements derived from the offshore GPS stations and ocean-bottom water pressure gauges (Sato *et al.*, 2011; Iinuma *et al.*, 2012) to better constrain the slip distribution in the shallow portion of the megathrust. Figure 1 shows the fault geometry and the distribution of stations we used. The fault consists of rectangular subfaults of varying sizes. The orientation of each subfault is fitted to the local strike and dip of the plate interface. The upper edge of the fault is set at a depth of 6.5 km beneath the axis of the Japan Trench. The lower edge of the fault is situated at a depth of 50 km, assuming the coseismic slip occur only at depths shallower than 50 km. In the dip direction, the boundaries of the subfaults are set at depths of 10, 15, 20, 30, and 40 km. The lengths of the subfaults in the strike direction range between 30 and 40 km. The total number of the subfaults is 132 with 6 segments in the dip direction and 22 segments in the strike direction.

We use the source code developed by Okada (1992) for the calculation of the static strains due to slip on the fault in a homogenous half-space medium. The Poisson ratio of the medium is assumed to be 0.25. Inversion of the deformation data for the subfault slips is done using the program system Statistical Analysis with Least-Squares Fitting, which was developed for nonlinear least-squares fitting in experimental sciences (Nakagawa and Oyanagi, 1980). Because of the difficulty in simultaneously resolving the slip amplitudes and rakes, we invert for only the slip amplitudes and fix the rakes at the values consistent with a motion direction of N70°W for the Pacific plate relative to the overriding plate. This value was chosen because it gave a better fit to the data than the N66°W direction, which is the motion of the Pacific plate relative to the North American plate estimated from the International Terrestrial Reference Frame 2005 global model (Altamimi *et al.*, 2007).

The determined slip distribution explains the observed data very well (Fig. 1). The summed moments of subfault slips give an M_w of 9.0 for a rigidity of 40 GPa. The subfault slips are characterized by two high-slip patches separated by a zone of relatively low slip. The 20 m slip contour exhibits two lobe-like patterns. Hereafter, we use the term "high-slip patch" and "high-slip lobe" interchangeably to indicate an area with slip greater than 20 m. Slip exceeds 60 m around the peaks of the two high-slip lobes. The crosses in Figure 2 denote the uncertainties of locations of the peaks, which are estimated based on the results of inversion performed for the subfaults with fault lengths half of the original ones. The peak of the northern high-slip lobe is located very close to the trench, coinciding with the sites where large seafloor displacements were observed (Fujiwara *et al.*, 2011; Ito *et al.*, 2011). The peak of the southern high-slip lobe is located about 40 km southeast of the mainshock epicenter, which is about 70 km away from the trench. The slip distribution of the 2011 Tohoku-Oki earthquake has been determined using similar geodetic data derived from both land and offshore stations (Iinuma *et al.*, 2012; Ozawa *et al.*, 2012). The slip distribution determined by Ozawa *et al.* (2012) is similar to ours in the sense that it is also characterized by two high-slip patches, although the locations of the peak slip in the two high-slip patches are slightly shifted toward the north relative to ours. The slip distribution determined by Iinuma *et al.* (2012) does not clearly exhibit two high-slip patches.

Seismicity during the Past 90 Years

Figure 2 shows the epicenter distribution of large events with the JMA magnitude (hereafter simply denoted as M unless otherwise stated) greater than 6.0 and 5.0 for the periods before and after the 2011 Tohoku-Oki earthquake, respectively. Generally, the large events are distributed away from the two high-slip patches both before and after the mainshock. The aftershocks near the trench are concentrated close to the peaks of the two high-slip patches. The stress change due to large slip near the trench is considered to have triggered normal-faulting events in the Pacific plate (Sato *et al.*, 2012). Figures 3 and 4 show a close up view of the JMA epicenters together with the rupture zones of several major earthquakes available in the literatures. There are three major clusters that are considered to be important for characterizing the spatiotemporal seismicity pattern in and around the two high-slip patches. First is a cluster of events located off the coast of Miyagi prefecture between the 30 and 50 km depth contours of the upper interface of the subducted Pacific plate. We call this cluster the "deep seismic activity" because it is distributed over the deep portion of the megathrust. The epicentral area of the deep seismic activity is included in the rupture zones of the 1936 and 1978 Off-Miyagi earthquakes, which had been regarded as the characteristic events for this region before the 2011 Tohoku-Oki earthquake. The rupture zones of the characteristic earthquakes do not overlap the southern high-slip patch. We find another cluster of events

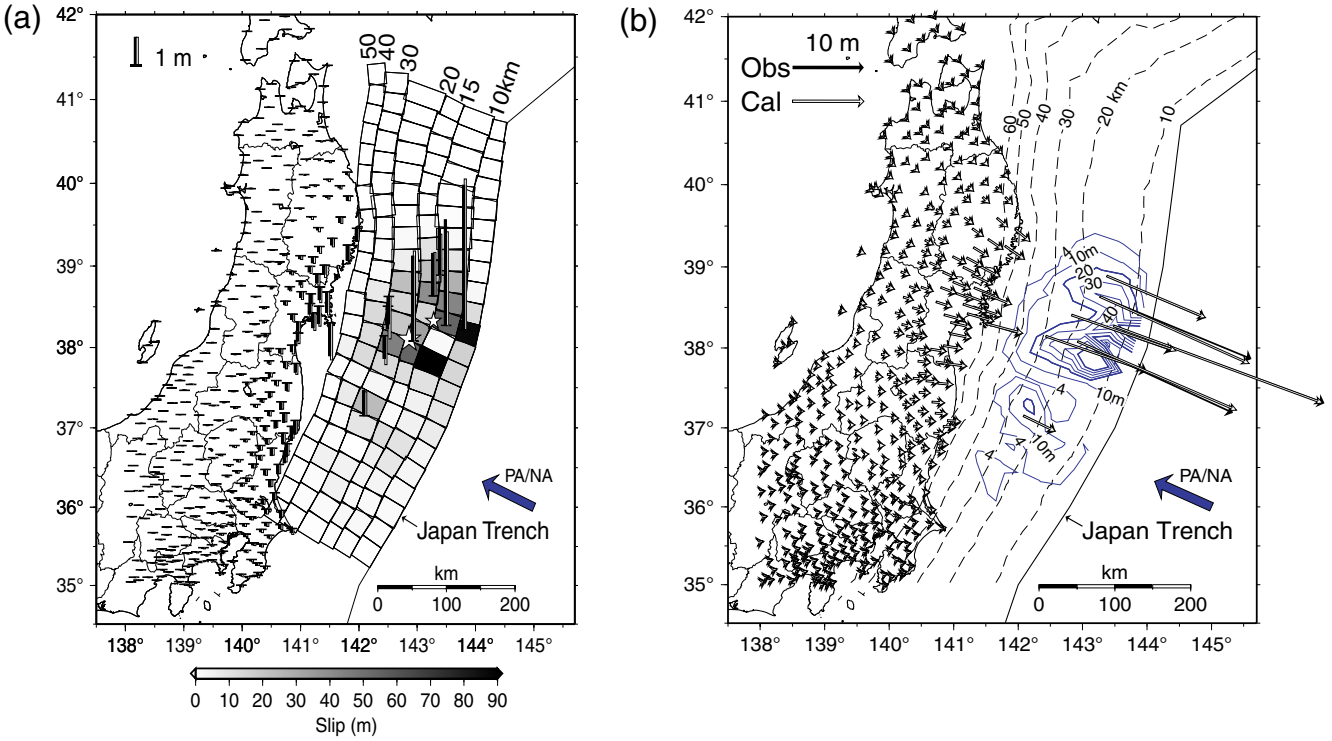

Figure 1. Comparison of observed (solid symbols) and calculated (open symbols) coseismic displacements for (a) vertical components and (b) horizontal components. In addition to the GEONET GPS stations, offshore GPS stations (KAMN, KAMS, MYGI, MYGW, FUKU) operated by the Japan Coast Guard, and offshore GPS and water pressure gauge stations (GJT3, GJT4, POP1, POP2, TJT1) operated by the Tohoku University are used. The geometry of the fault is shown in (a). The slip distribution is indicated by the contour lines in (b). The contour interval is 10 m for the slip ≥10 m. The large and small stars denote the epicenters of the Tohoku-Oki earthquake and the M 7.3 foreshock on 9 March 2011, respectively. The broken lines show the depth of the upper interface of subducted Pacific plate. The thick arrow indicates the direction of motion of the Pacific plate relative to the North American plate. The color version of this figure is available only in the electronic edition.

near the epicenters of the M 7.3 foreshock that occurred two days before the mainshock. The cluster is distributed in the range between the 10 and 20 km depth contours of the upper interface of the subducted Pacific plate. We call this cluster the "shallow seismic activity" as it represents seismic activity in the shallow portion of the megathrust. The shallow seismic activity is distributed in the western edge of the northern high-slip patch and also along the eastern edge of the rupture zone of the 1981 M 7.0 earthquake. Finally, though it is not very clear as the previous two features, we find a cluster of events located near the mainshock epicenter, extending along the 20 km depth contour of the upper interface of the subducted Pacific plate. We call this cluster the "midseismic activity" because the seismic activity is located halfway between the deep and shallow portions of the megathrust. The southern high-slip patch is divided into western and eastern parts by the midseismic activity. The depth contours of the plate interface indicate the dip of the plate interface changes rapidly around at the depth of 20 km. The midseismic activity is included in the rupture zone of the 2003 M 6.8 earthquake that almost overlaps the western half of the southern high-slip patch.

Figure 5 shows the plot of epicenters in latitude against time for the large events ($M \geq 6.0$). In addition to the foreshock activity and the 1981 event, we find two other prominent events in the zone of shallow seismic activity during 1939 and 1958. Dividing the time span into four periods, P1 to P4, we describe the spatiotemporal seismicity pattern in detail for the times including those prominent events. The outline of the following description is listed in Table 1.

Period P1 (1923–1947; Figure 6a)

The 1939 activity in the zone of shallow seismic activity consists of five large earthquakes ($M \geq 6.0$). Three of the events initially occurred in the northern part of the zone. They were followed about 10 months later by an earthquake of M 6.9 in the southern part, which is the largest for the 1939 events. The 1939 event was preceded three years earlier by a large M 7.4 earthquake in the zone of deep seismic activity, which is named the 1936 Miyagi-Oki earthquake. Although the epicenters of earthquakes in 1933 (M 7.1) and 1937 (M 7.1) are located close to the 1936 Miyagi-Oki earthquake, they are thought to be a shallow event within the overriding plate and an intraplate earthquake within the subducted slab, respectively (Kanamori *et al.*, 2006). To the south of the southern high-slip patch, a strong swarm activity

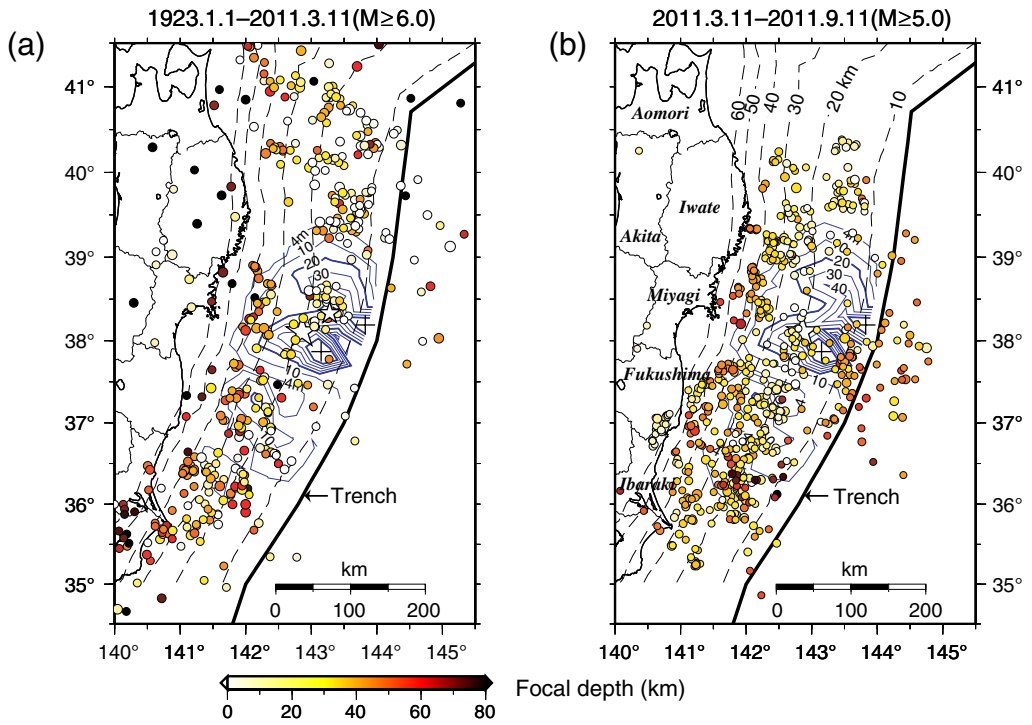

Figure 2. The epicenter distribution of events (a) before and (b) after the 2011 Tohoku-Oki earthquake. The large and small stars indicate the epicenters of the Tohoku-Oki earthquake and the *M* 7.3 foreshock on 9 March 2011, respectively. The slip distribution of the Tohoku-Oki earthquake is shown by the contours at an interval of 10 m. The minimum slip contour is 4 m. The region with slip greater than 20 m is defined as the high-slip patch. The crosses denote the peaks of the two high-slip patches where the slip exceeds 60 m. The broken lines indicate the depth of the upper interface of subducted Pacific plate. The color version of this figure is available only in the electronic edition.

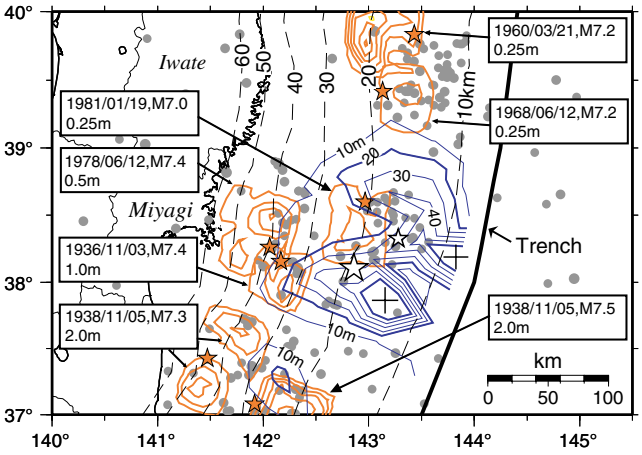

Figure 3. The epicenter distribution of events ($M \geq 6.0$) from 1923 until just before the 2011 Tohoku-Oki earthquake, superimposed on the slip distribution of the Tohoku-Oki earthquake. The slip distributions of major interplate earthquakes available in the literature are also shown for the events before 2003 from Yamanaka and Kikuchi (2004) and Murotani *et al.* (2004). The interval of slip contour is indicated for each event. The small stars denote the JMA epicenters of the major interplate earthquakes. The large star indicates the epicenter of the Tohoku-Oki earthquake. The color version of this figure is available only in the electronic edition.

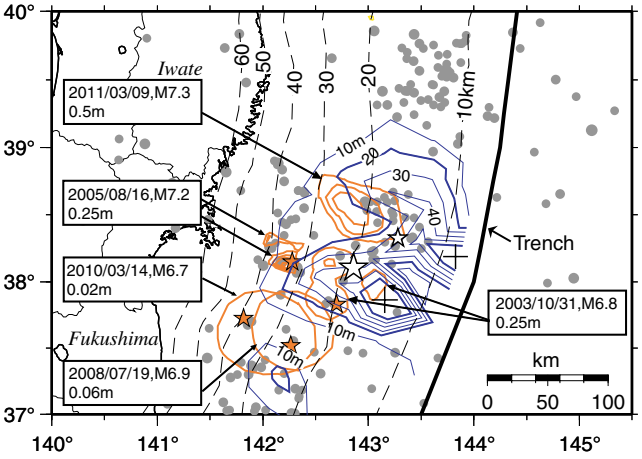

Figure 4. The epicenter distribution of events ($M \geq 6.0$) from 1923 until just before the 2011 Tohoku-Oki earthquake, superimposed on the slip distribution of the Tohoku-Oki earthquake. The slip distributions of major interplate earthquakes available in the literature are also shown for the events after 2003 from Yamanaka (the EIC Note, see Data and Resources), Suito *et al.* (2011), and Shao, Ji, and Zhao (2011). The interval of slip contour is indicated for each event. The small stars denote the JMA epicenters of the major interplate earthquakes. The large star indicates the epicenter of the Tohoku-Oki earthquake. The color version of this figure is available only in the electronic edition.

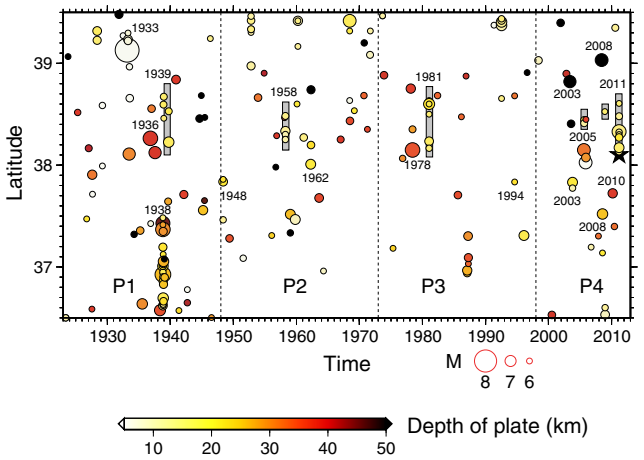

Figure 5. Spatiotemporal distribution of events ($M \geq 6.0$) in the range of latitude 36.5°–39.5° N and longitude 140.0°–145.5° E. The bars indicate the prominent seismic activity in the zone of shallow seismic activity. The star indicates the mainshock of the 2011 Tohoku-Oki earthquake. The events are shaded according to the depth of the upper interface of the subducted Pacific plate beneath the epicenter of an event. The events located on land are shown by black circles. The color version of this figure is available only in the electronic edition.

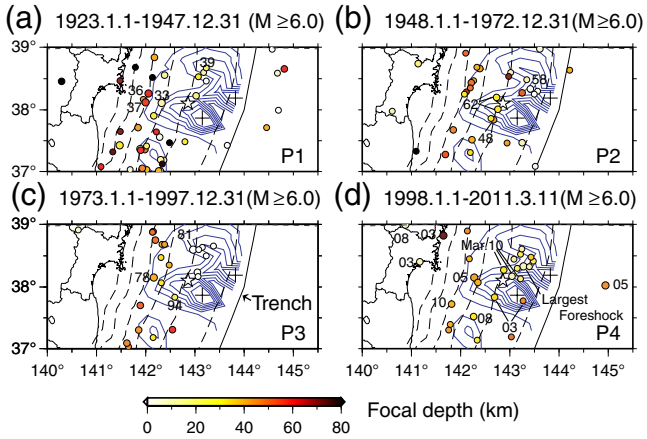

Figure 6. The epicenter distribution of events ($M \geq 6.0$) for the periods P1 to P4 indicated in Figure 5. The star indicates the mainshock epicenter. The slip of the Tohoku-Oki earthquake is denoted by the contours at 10 m intervals. The crosses denote the peaks of high-slip patches. The broken lines indicate the depths of the upper interface of subducted Pacific plate every 10 km. The numbers attached to selected events indicate the last two digits of the year. Mar.10 indicates the 10 March 2011 (JST) event. The color version of this figure is available only in the electronic edition.

(including four $M > 7.0$ earthquakes) occurred off the coast of Fukushima prefecture in 1938. To the north of the northern high-slip patch, the great 1933 Sanriku-Oki earthquake (M 8.4) occurred in the outer-rise region off the coast of Iwate prefecture (Fig. 5).

Period P2 (1948–1972; Figure 6b)

The 1958 activity in the zone of the shallow seismic activity consists of five large earthquakes ($M \geq 6.0$) with the largest of M 6.7. This event was not preceded by any $M \geq 7$ earthquakes in the zone of deep seismic activity. The midseismic activity is unusually high during this period. Two earthquakes (M 6.6 and M 6.1) occurred in the southern area in 1948, and two other earthquakes (M 6.8 and M 6.4) occurred in the northern area in 1962. Thereafter, no large earthquakes occurred in the zone of midseismic activity until 1994.

Period P3 (1973–1997; Figure 6c)

The 1981 activity includes the second largest earthquake (M 7.0) to have ever occurred in the zone of shallow seismic activity. The epicenter of the M 7.0 earthquake is located at the northern end of the rupture zone, which extends over an area of relatively low slip sandwiched between the two high-slip patches (Fig. 3). The M 7.0 earthquake was followed four days later by two earthquakes (M 6.6 and M 6.2) in the southern part of the same seismic zone. This migration of seismic activity from north to south within the zone of shallow seismic activity is similar to that during the 1939 activity. Moreover, as the 1939 event was preceded by the 1936 Miyagi-Oki earthquake, the 1981 event was preceded three years earlier by an earthquake of M 7.4, which is named the 1978 Miyagi-Oki earthquake, in the zone of deep seismic activity. The rupture zone of the 1978 Miyagi-Oki earthquake is estimated to be located slightly down-dip of the 1936 earthquake (Yamanaka and Kikuchi, 2004). The

Table 1
Spatiotemporal Seismicity Pattern

	Deep Seismic Activity	Shallow Seismic Activity	Midseismic Activity	Off Fukushima Activity
Period PI (1923–1947)	1936 (M 7.4)	1939 (Five $M \geq 6.0$, $M_{max} = 6.9$) north to south migration		1938 Swarm ($M > 7.0$)
Period P2 (1948–1972)	None	1958 (Five $M \geq 6.0$, $M_{max} = 6.7$)	I948 (M 6.6. M 6.1) 1962 (M 6.8. M 6.4)	
Period P3 (1973–1997)	1978 (M 7.4)	1981 (Six $M \geq 6.0$, $M_{max} = 7.0$) north to south migration	1994 (M 6.0)	
Period P4 (1998–2011)	2005 (M 7.2)	2005 (M 6.3, M 6.3) 2008 (M 6.I) 2011 (Eight $M \geq 6.0$, $M_{max} = 7.3$) north to south migration	2003 (M 6.8. M 6.3)	2008 (M 6.9) 2010 (M 6.7)

seismicity in the zone of midseismic activity was low during this period. We find only one earthquake (M 6.0) that occurred in the southern area in 1994.

Period P4 (1998–2011; Figure 6d)

In addition to the foreshock activity in 2011, we find two other less prominent events occurring in the zone of shallow seismic activity. They are the 2005 activity consisting of two M 6.3 earthquakes and a single M 6.1 earthquake in 2008 (Fig. 5). The 2005 activity was also preceded by an earthquake of M 7.2 in the zone of deep seismic activity. The lead time is nine days, which is much shorter than the three years for the previous two cases. Quite interestingly, the 2005 activity in the zone of shallow seismic activity was followed three months later by an M 7.2 normal-faulting earthquake in the outer rise near the peak of the northern high-slip patch. Before the Tohoku-Oki earthquake, this event was the largest to have ever occurred in the outer-rise off the coast of Miyagi and Fukushima prefectures. (Later, a normal-faulting earthquake of M 7.5 occurred in the same area 40 min after the Tohoku-Oki earthquake.) Half a month later, the 2005 normal-faulting earthquake was in turn followed by another large earthquake (M 6.6) in the zone of deep seismic activity. In a short period of time, a number of large earthquakes occurred surrounding the southern high-slip patch, migrating from the zone of deep seismic activity via the zone of shallow seismic activity to the outer rise and again back to the zone of deep seismic activity. According to Kanamori *et al.* (2006), the size of the 2005 M 7.2 earthquake in the zone of deep seismic activity is 3–4.5 times smaller than that of the 1978 Miyagi-Oki earthquake, whereas both the size and location of the 2005 M 7.2 earthquake are estimated to be the same as the 1936 Miyagi-Oki earthquake. According to Yamanaka (Earthquake Information Center [EIC] Notes; see Data and Resources), the rupture zone of the 2005 earthquake is estimated to be located up-dip relative to the 1978 earthquake and toward the north relative to the 1936 earthquake (Figs. 3 and 4). It appears the rupture zones of the 1936 and the 2005 earthquakes are located significantly up-dip relative to the 1978 earthquake.

Prior to the series of large events in 2005, an M 6.8 event occurred in the zone of midseismic activity in 2003. The rupture zone of the earthquake is located up-dip of the rupture zones of the 1936 and 2005 earthquakes, coinciding with the western part of the southern high-slip patch (Fig. 4). The M 6.8 earthquake was followed a day and a half later by a second earthquake of M 6.3 that occurred about 50 km to the east. We find no other large earthquakes in this location for the entire period of time (Fig. 1). On the other hand, we find the M 6.6 earthquake of 1948 (Fig. 6b) and the M 6.0 earthquake of 1994 (Fig. 6c) are located very close to the epicenter of the M 6.8 earthquake. The overlapping source areas suggest that some local fault structure responsible for generating those events persisted for a long period of time, and JMA epicenters have fairly good accuracies since early times. While the 2003 earthquake was followed by the series of large earthquakes in 2005, the 1948 and 1994 earthquakes were not followed by any prominent seismic activities in the surrounding area.

The M 7.3 foreshock that occurred two days (51 hrs) before the mainshock is the largest to have ever occurred in the zone of shallow seismic activity. Although its epicenter is located a few tens of km south of the epicenter of the 1981 M 7.0 earthquake, the rupture zones of the two earthquakes are estimated to be almost the same (Shao, Ji, and Zhao, 2011). The foreshock activity migrated toward the epicenter of the mainshock in the two days before the mainshock (Ando and Imanishi, 2011; Kato *et al.*, 2012). This is similar to the migrations of seismic activity from north to south found during the 1939 and 1981 events. The epicenters of three large earthquakes (M 6.4, M 6.3, and M 6.8) that occurred between 35 and 32 hrs before the mainshock (March 10 JST) are distributed on the northern edge of the southern high-slip patch. According to Ohta *et al.* (2012), the largest foreshock was followed by afterslip equivalent to an M_w 6.8 event. The estimated coseismic and afterslip distributions are complementary, the afterslip being distributed south of the coseimic slip, which is consistent with the migration of the foreshock activity from north to south.

The seismicity off the coast of Fukushima prefecture started to increase around 2006 (Fig. 5). The largest events are an M 6.9 earthquake in 2008 and an M 6.7 earthquake in 2010. According to Suito *et al.* (2011), the rupture zones of these earthquakes extend close to the southern high-slip patch (Fig. 4). These earthquakes are followed by unusually large afterslip in comparison with other interplate earthquakes. The large earthquakes mentioned so far for the period P4 all have the focal mechanisms consistent with the underthrusting motion of the Pacific plate relative to the overriding plate, except the normal faulting earthquake that occurred in the outer rise in 2005 (Asano *et al.*, 2011).

The seismic activity on land west of the two high-slip patches was significantly high during 2003. Shortly before the M 6.8 earthquake (October 31) in the zone of midseismic activity, two large earthquakes occurred near the coast of Miyagi prefecture. One is a deep M 7.1 earthquake within the subducted slab (May 26), and the other is a shallow M 6.4 earthquake within the overriding plate (July 26). Five years later, a shallow M 7.2 event occurred near the border of Iwate–Miyagi–Akita prefectures in 2008. These onshore earthquakes are indicated by black circles in Figure 5.

Figure 7 shows the distribution of $M \geq 4.0$ earthquakes for several selected time windows from the time of the 2003 event until just before the mainshock. Figure 8 shows all the epicenters for all time windows in Figure 7. Including these smaller events, we can see more details of the seismicity pattern. For example, we find an east–west trending cluster extending between the epicenters of the M 6.8 and M 6.3 earthquakes in 2003 (Fig. 7a). Actually, the largest foreshock on 9 March 2011 was preceded by moderate seismic activity located up-dip of the foreshock epicenter near the peak of the

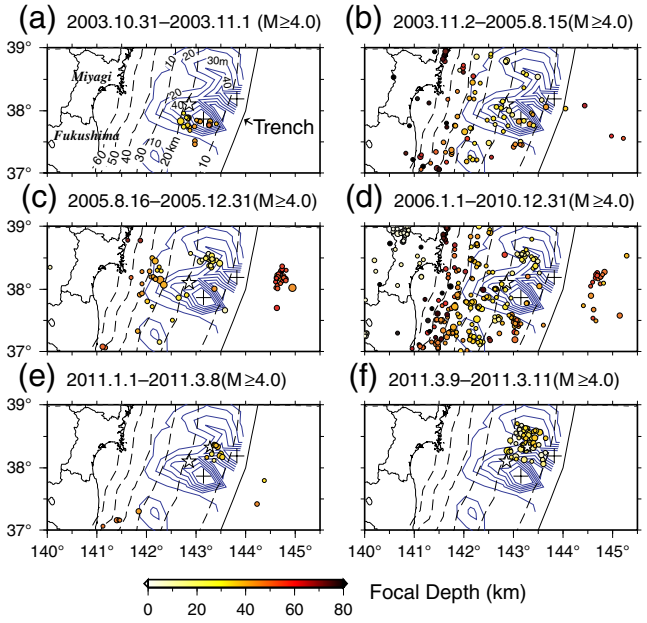

Figure 7. (a–f) The epicenter distribution of events ($M \geq 4.0$) for the selected time windows from the start of the 2003 activity until just before the occurrence of the Tohoku-Oki earthquake. The large and small stars indicate the epicenters of the mainshock and the largest foreshock, respectively. The slip of the Tohoku-Oki earthquake is shown by the contours at 10 m intervals. The crosses indicate the peaks of the two high-slip patches. The broken lines indicate the depth of the upper interface of the subducted Pacific plate every 10 km. The color version of this figure is available only in the electronic edition.

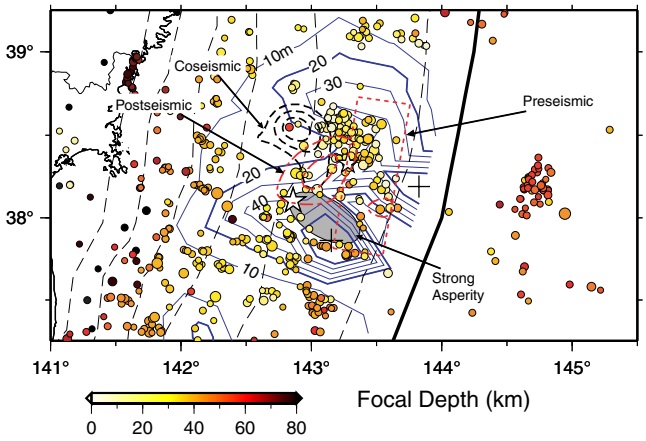

Figure 8. The epicenter distribution of $M \geq 4.0$ events for the period from the start of the 2003 activity until just before the occurrence of the Tohoku-Oki earthquake (31 October 2003–11 March 2011). The large and small stars indicate the epicenters of the mainshock and the largest foreshock, respectively. The slip of the Tohoku-Oki earthquake is shown by the contours at 10 m intervals. The crosses denote the peaks of the two high-slip patches. The broken lines indicate the depth of the upper interface of the subducted Pacific plate every 10 km. The coseismic and postseismic slips of the largest foreshock are from Ohta *et al.* (2012). The contours are 0.5, 1.0, and 1.5 m for the coseismic slip and 0.3 and 0.4 m for the postseismic slip. The broken rectangle shows the zone of slow-slip event prior to the largest foreshock (Ito *et al.*, 2013). The strong patch (asperity) surrounded by the doughnut-shaped seismicity pattern is indicated by the gray ellipse. The color version of this figure is available only in the electronic edition.

northern high-slip patch (Fig. 7e). The seismic activity was accompanied by a slow-slip event (M_w 7.0) located up-dip of the foreshock epicenter (Ito *et al.*, 2013). The epicenters of the foreshock activity can be divided into three subclusters, one containing the epicenter of the largest foreshock, another close to the peak of the northern high-slip patch, and the last extending along the northern edge of the southern high-slip patch (Fig. 7f). In Figure 8, we superimposed the zone of the slow-slip event (Ito *et al.*, 2013) and the zones of coseismic and postseismic slips of the largest foreshock determined by Ohta *et al.* (2012). The three subclusters are generally distributed near the edges of those zones. Lastly, we find an elliptical region surrounded by a significant number of earthquakes near the peak of the southern high-slip patch. It is similar to the doughnut-shaped seismicity pattern found by Mogi (1969) for several large earthquakes in and around Japan. A similar seismicity pattern can be seen in the same region for the epicenter distribution of large event ($M \geq 6.0$) since 1923 (Fig. 2a). The doughnut-shaped seismicity pattern may have been produced by the stress concentration created along the edge of a strong asperity. The asperity was so strong that it had not ruptured during surrounding large earthquakes for a long period of time.

Lastly, we briefly describe the epicenter distribution of aftershocks for the period of six months after the mainshock (Fig. 2b). Only few aftershocks are found in the zone of shallow seismic activity. On the other hand, many aftershocks are found in the zone of midseismic activity where the seismicity had been relatively low, compared with those in the zones of deep and shallow seismic activities. Also, many aftershocks are distributed along the trench near the peaks of the two high-slip patches. Near the peak of the southern high-slip patch, more aftershocks are distributed between the peak of the southern high-slip patch and the trench. In the north, the aftershocks are distributed mainly over the outer rise, circumventing the peak of the northern high-slip patch. These observations strongly support the idea that the slip distribution is characterized by two high-slip patches with their peaks located at different distances from the trench. Figure 9 shows the epicenter distribution of aftershocks with $M \geq 4.0$. We find the aftershocks are distributed bounding the asperity derived from the seismicity pattern before the Tohoku-Oki earthquake. Because most of these aftershocks have the focal mechanisms inconsistent with the underthrusting motion of the Pacific plate relative to the overriding plate (Asano *et al.*, 2011; Nettles *et al.*, 2011), the aftershock distribution suggests the effect of the slip distribution characterized by the two high-slip patches reaches beyond the plate interface and influences intraplate events of the overriding plate and subducted Pacific plate.

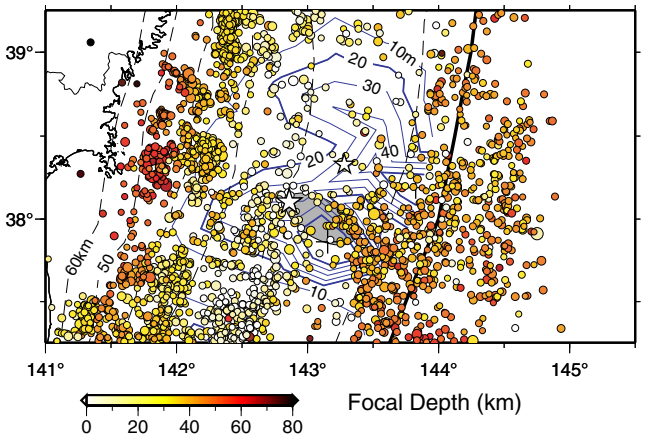

Figure 9. The epicenter distribution of $M \geq 4.0$ events for the period of six months after the Tohoku-Oki earthquake (11 March 2011–11 September 2011). The large and small stars indicate the epicenters of the mainshock and the largest foreshock, respectively. The slip of the Tohoku-Oki earthquake is shown by the contours at 10 m intervals. The crosses denote the peaks of the two high-slip patches. The broken lines indicate the depth of the upper interface of the subducted Pacific plate every 10 km. The asperity derived from the seismicity pattern before the Tohoku-Oki earthquake is indicated by the gray ellipse. The color version of this figure is available only in the electronic edition.

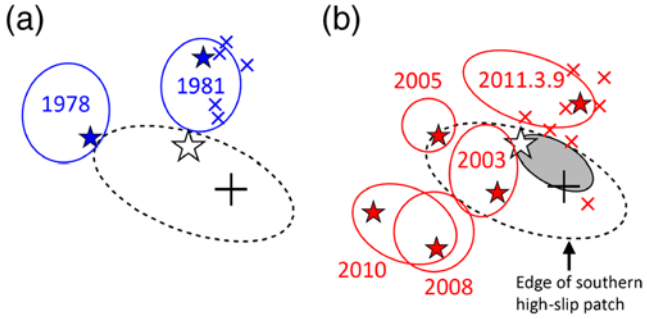

Figure 10. A schematic illustration showing the different conditions between (a) the time prior to the 1981 activity and (b) the time prior to the 2011 Tohoku-Oki earthquake. The large open star indicates the mainshock epicenter. The rupture zones of the 1981 event (M 7.0) and the 2011.3.9 foreshock (M 7.3) are from Yamanaka and Kikuchi (2004) and Shao, Ji, and Zhao (2011), respectively. The rupture zones of the 2003 M 6.8 and 2005 M 7.2 events are from the EIC Note by Yamanaka (see Data and Resources). The rupture zones of the 2008 (M 6.9) and 2010 (M 6.7) events are from Suito *et al.* (2011). The crosses indicate the $M \geq 6.0$ events around the southern high-slip patch. The large cross indicates the location of slip peak. The gray ellipse indicates the strong asperity estimated from the seismicity pattern before the Tohoku-Oki earthquake. The color version of this figure is available only in the electronic edition.

Implications for the Mainshock Rupture Process

According to Ide *et al.* (2011) and Shao *et al.* (2011), the 2011 Tohoku-Oki earthquake nucleated about 150 km off the coast of Miyagi prefecture and propagated down-dip toward the deeper half of the megathrust for the first 50 s. Then it expanded to shallower depths for the next 40 s, with the largest slip along the fault occurring more than 150 km offshore close to the trench. Thereafter, the rupture propagated again down-dip toward the deeper half of the megathrust and finally moved toward the south. The mainshock nucleated near the northern edge of the zone of midseismic activity. With reference to the slip distribution, the rupture area for the first 50 s corresponds to the region including the western half of the southern high-slip patch and the zone of deep seismic activity. The rupture zone for the next 40 s covers the eastern half of the southern high-slip patch and its surroundings.

Based on the spatiotemporal seismicity pattern of the previous 90 years described in the Seismicity during the Past 90 Years section, we consider that two rare events occurred during the sequence of foreshocks and mainshock. One is that the shallow seismic activity led to rupture in the down-dip portion of the megathrust, including the western half of the southern high-slip patch and the zone of deep seismic activity. Previously, none of the three prominent events (1939, 1958, and 1981 events) in the zone of shallow seismic activity triggered rupture of the down-dip portion of the megathrust. Second, the rupture in the down-dip portion of the megathrust during the mainshock triggered a massive rupture in the up-dip portion, corresponding to the eastern half of the southern high-slip patch. The 2003 M 6.8 earthquake that ruptured the western half of the southern high-slip patch might have had a chance for that but failed. Although large earthquakes in the zone of deep seismic activity preceded the prominent seismic activities in the zone of shallow seismic activity in a few sequences (1939, 1981, and 2005), they never induced a large rupture in the region of the eastern half of the southern high-slip patch.

In order to address the question, why a great earthquake like the 2011 Tohoku-Oki earthquake was not triggered by previous M 6 and 7 earthquakes that occurred in the same epicentral area as the foreshock activity, we illustrate the distribution of major earthquakes prior to the foreshock activity and the 1981 event in Figure 10. The 1981 event consists of six $M \geq 6.0$ events with the largest one of M 7.0, while the 2011 foreshock activity consists of eight $M \geq 6.0$ events with the largest one of M 7.3. In total, the size of the foreshock activity is significantly larger than that of the 1981 event. The 1981 event was preceded by the 1978 Miyagi-Oki earthquake in the zone of deep seismic activity, whereas the foreshock activity was preceded by the 2005 Miyagi-Oki earthquake in the zone of deep seismic activity. The 2005 earthquake is estimated to be 3–4.5 times smaller than the 1978 earthquake (Kanamori *et al.*, 2006), but its effect on the western half of the southern high-slip patch might not have been less than the 1978 earthquake because its rupture zone is located closer to the western half than the 1978 earthquake (Yamanaka and Kikuchi, 2004). While the foreshock activity was preceded by an M 6.8 earthquake in the zone of midseismic activity and an M 6.3 earthquake near the peak of the southern high-slip patch in 2003, the 1981 event was not preceded by any such events. Furthermore, while the

foreshock activity was preceded by the 2008 and 2010 earthquakes located south of the southern high-slip patch, the 1981 event was also not preceded by any large earthquakes in that region. Based on these differences, it is inferred that the state of stress before the 2011 foreshock activity was better conditioned for rupturing the southern high-slip patch than the 1981 event.

The activities in 1939 and 1958 were also quite different from the 2011 foreshock activity. The 1939 activity was not preceded by any large earthquake in the zone of midseismic activity and near the peak of the southern high-slip patch. The 1958 activity was not preceded by any large earthquakes in the zone of deep seismic activity (Table 1).

From comparison of the 1939, 1958, 1981, and 2011 sequences, we suggest the events in 2003 of an M 6.8 earthquake in the zone of midseismic activity and an M 6.3 earthquake near the peak of the southern high-slip patch played an important role related to the Tohoku-Oki earthquake. Based on the long-term seismicity described in the Seismicity during the Past 90 Years section, we propose the foreshock activity was able to trigger the Tohoku-Oki earthquake because the increased stress from the foreshock activity was able to overcome the strength of the southern high-slip patch that had been sufficiently weakened by the series of large events in its surroundings since 2003. In previous decades, prominent events in the zone of shallow seismic activity were not able to trigger such a great earthquake because a similar stress condition had not been established.

Because the mainshock epicenter is located at the northern edge of the midseismic activity that divides the southern high-slip patch into the western and eastern halves, it seems likely that the eastern half of the southern high-slip patch would rupture first. Probably, this did not occur because the eastern half of the southern high-slip patch was much stronger than the western half, as is estimated from the difference in the slip amount between the two halves. The eastern half was in such a state that its rupture could only be triggered dynamically following the rupture of the western half. The extremely large slip near the peak of the southern high-slip patch induced the rupture over a large adjacent region, including the peak of the northern high-slip patch close to the trench, thus making a great earthquake of M_{w} 9.0.

Discussion

GEONET stations located in the coastal area to the west of the southern high-slip patch demonstrated crustal deformations suggesting a decrease in the plate coupling after the 2003 M 6.8 event (Ozawa *et al.*, 2012). The trend declined but increased again after the 2005 event in the zone of deep seismic activity, then continued through the following period until the occurrence of the foreshock activity in 2011. This suggests a large-scale slow slip taking place prior to the Tohoku-Oki earthquake in the vicinity of the high-slip patches. The analysis of tidal triggering of earthquakes indicates the stress in the hypocentral area of the Tohoku-Oki earthquake increased since 2003 (Tanaka, 2012). These observations are not inconsistent with our inference that the southern high-slip patch had been greatly weakened by the series of large surrounding earthquakes since 2003. The subduction rate of the Pacific plate appears to have increased immediately after the occurrence of the 2003 M 8.0 Tokachi-Oki earthquake in the adjacent plate boundaries (Heki and Mitsui, 2013). The 2003 M 6.8 earthquake in the midseismic zone occurred about a month after the Tokachi-Oki earthquake. It is interesting to speculate whether the 2003 event with an epicentral distance of about 500 km was induced by the Tokachi-Oki earthquake.

The rupture zones of the largest foreshock and the 1981 earthquake are distributed over the relatively low-slip zone sandwiched between the two high-slip patches of the 2011 Tohoku-Oki earthquake (Figs. 3 and 4). Probably, the repetitive occurrence of similar M 7 class earthquakes in the past has reduced the slip deficit in that zone, thereby yielding the low-slip zone between the two high-slip patches during the Tohoku-Oki earthquake. As mentioned earlier, the epicenters in the zone of shallow seismic activity are divided into three subclusters. The subclusters are not distributed close to the centers of the preseismic, coseismic, and postseismic slip zones of the largest foreshock (Ohta *et al.*, 2012; Ito *et al.*, 2013), suggesting the earthquakes in this region nucleate near the boundary between the zones with different frictional properties on the megathrust. We found three cases in which the earthquake activity migrated from north to south within the zone of shallow seismic activity (Table 1). We also found three cases in which the shallow seismic activity is preceded by the deep seismic activity by lead times in the range of three years to nine days (Table 1). These repeated migrations of seismic activities suggest some governing mechanism persisting for periods of up to several years, which perhaps involves the heterogeneous frictional properties on the megathrust. With the improvement of geodetic measurements, many aseismic events are known to have occurred before the 2011 Tohoku-Oki earthquake (Suito *et al.*, 2011; Ohta *et al.*, 2012; Ozawa *et al.*, 2012; Ito *et al.*, 2013). It is not known whether these aseismic events are common because it is difficult to identify such events using older geodetic data.

The V_P/V_S ratio derived from tomographic studies for the lower portion of the overriding plate suggests the rupture zones of the 1981 earthquake and the largest foreshock are structurally different from the surrounding area (Shao, Ji, and Zhao, 2011). Also, the heterogeneities of P-wave velocities for the lower portion of the overriding plate (Zhao *et al.*, 2011) show a good correlation with the distribution of the two high-slip patches. A precise tomographic image determined using the data combining ocean-bottom seismographs and land seismic stations (Yamamoto *et al.*, 2013) reveals a north–south elongated patch of low V_S and high V_P/V_S ratio in the subducted oceanic crust that covers the zone of midseismic activity. The structural heterogeneities close to the megathrust plate boundary appear to be related to the slip distribution of the Tohoku-Oki earthquake and the distribution of earthquakes for the past 90 years.

Conclusions

This study shows a slip distribution characterized by two high-slip patches separated by a zone of relatively low slip, which is correlated to the seismicity over the past 90 years. From these data, we suggest the foreshock activity was able to trigger the mainshock because the southern high-slip patch had been sufficiently weakened by a series of large events since 2003. Significant earthquakes during the previous decades did not trigger a great earthquake because the regional stress conditions were different. During the 2011 mainshock, the detailed stress distribution at that time enabled large slip in the southern high-slip patch to induce subsequent rupture of large adjacent regions, including the northern high-slip patch. Seismicity patterns such as the doughnut surrounding the peak of the southern high-slip patch, suggest areas of high strength that had not ruptured at least during the past 90 years.

The long-term seismicity shows other characteristic features of seismicity that can be related to the slip distribution of the Tohoku-Oki earthquake. The distribution of the earthquake subclusters in relation to the zones of preseismic, coseismic, and postseismic slips of the largest foreshock suggests the earthquakes tend to nucleate near the boundary between different regions that have varying frictional behaviors. The repetitive occurrences of similar migration of seismic activity suggest a persistent mechanism that involves the heterogeneous distribution of frictional properties on the megathrust. The structural heterogeneities near the megathrust plate boundary appear to be correlated with the slip distribution of the Tohoku-Oki earthquake and the long-term seismicity. The 2011 M_w 9.0 Tohoku-Oki has provided us with an unprecedented opportunity for understanding the relationship between the heterogeneous distribution of frictional properties on the megathrust and the seismic activity.

Data and Resources

Information was used from Yamanaka's EIC Note, available at http://www.eri.u-tokyo.ac.jp/sanchu/Seismo_Note/EIC_News/031031.html (last accessed February 2013) for the 2003 M 6.8 event, and from http://www.eri.u-tokyo.ac.jp/sanchu/Seismo_Note/2005/EIC168.html for the 2005 M 7.2 event (last accessed February 2013).

Acknowledgments

We are grateful to the Geospatial Information Authority of Japan (GSI) for the GEONET GPS data and to the Japan Coast Guard and Tohoku University for the offshore geodetic data derived from GPS and water pressure gauges. We thank Y. Yamanaka, S. Murotani, H. Suito, G. Shao, and Y. Ohta for providing slip data. We thank Y. Okada for providing the source code for calculating the elastic deformation due to dislocation in a half-space. The figures are prepared using Generic Mapping Tools (Wessel and Smith, 1991). We thank anonymous reviewers for the comments that were helpful in revision of the manuscript.

References

Altamimi, Z., X. Collilieux, J. Legrand, B. Garayt, and C. Boucher (2007). ITRF 2005: A new release of the international terrestrial reference frame based on time series of station positions and earth orientation parameters, *J. Geophys. Res.* **112,** no. B09401, doi: 10.1029/2007JB004949.

Ando, R., and K. Imanishi (2011). Possibility of M_w 9.0 mainshock triggered by diffusional propagation of after-slip from M_w 7.3 foreshock, *Earth Planets Space* **63,** 767–771, doi: 10.5047/eps.2011.05.016.

Asano, Y., T. Saito, Y. Ito, K. Shiomi, H. Hirose, T. Matsumoto, S. Aoi, S. Hori, and S. Sekiguchi (2011). Spatial distribution and focal mechanisms of aftershocks of the 2011 off the Pacific coast of Tohoku earthquake, *Earth Planets Space* **63,** 669–673, doi: 10.5047/eps.2011.06.016.

Earthquake Research Committee (ERC) (2009). *Long-term Forecast of Earthquakes from Sanriku-Oki to Boso-Oki* (revised), Headquarters of Earthquake Research Promotion, Tokyo, Japan, 80 pp. (in Japanese).

Fujii, Y., K. Satake, S. Sakai, M. Shinohara, and T. Kanazawa (2011). Tsunami source of the 2011 off the Pacific coast of Tohoku, Japan earthquake, *Earth Planets Space* **63,** 815–820, doi: 10.5047/eps.2011.06.010.

Fujiwara, T., S. Kodaira, T. No, Y. Kaiho, N. Takahashi, and Y. Kaneda (2011). The 2011 Tohoku-Oki earthquake: Displacement reaching the trench axis, *Science* **334,** 1240, doi: 10.1126/science.1211554.

Heki, K., and Y. Mitsui (2013). Accelerated pacific plate subduction following interplate thrust earthquakes at the Japan trench, *Earth Planet. Sci. Lett.* **363,** 44–49.

Ide, S., A. Baltay, and G. C. Beroza (2011). Shallow dynamic overshoot and energetic deep rupture in the 2011 M_w 9.0 Tohoku-Oki earthquake, *Science* **332,** 1426–1429, doi: 10.1126/science.1207020.

Iinuma, T., R. Hino, M. Kido, D. Inazu, Y. Osada, Y. Ito, M. Ohzono, H. Tsushima, S. Suzuki, H. Fujimoto, and S. Miura (2012). Coseismic slip distribution of the 2011 Off the Pacific coast of Tohoku earthquake (M 9.0) refined by means of seafloor geodetic data, *J. Geophys. Res.* **117,** no. B07409, doi: 10.1029/2012JB009186.

Ito, Y., R. Hino, M. Kido, H. Fujimoto, Y. Osada, D. Inazu, Y. Ohta, T. Iinuma, M. Ohzono, S. Miura, M. Mishina, K. Suzuki, T. Tsuji, and J. Ashi (2013). Episodic slow slip events in the Japan subduction zone before the 2011 Tohoku-Oki earthquake, *Tectonophysics* **600,** 14–26.

Ito, Y., T. Tsuji, Y. Osada, M. Kido, D. Inazu, Y. Hayashi, H. Tsushima, R. Hino, and H. Fujimoto (2011). Frontal wedge deformation near the source region of the 2011 Tohoku-Oki earthquake, *Geophys. Res. Lett.* **38,** L00G05, doi: 10.1029/2011GL048355.

Kanamori, H., M. Miyazawa, and J. Mori (2006). Investigation of the earthquake sequence off Miyagi prefecture with historical seismograms, *Earth Planets Space* **58,** 1533–1541.

Kato, A., K. Obara, T. Igarashi, H. Tsuruoka, S. Nakagawa, and N. Hirata (2012). Propagation of slow slip leading up to the 2011 M_w 9.0 Tohoku-Oki earthquake, *Science* **335,** 705–708, doi: 10.1126/science.1215141.

Lay, T., C. J. Ammon, H. Kanamori, L. Xue, and M. J. Kim (2011). Possible large near-trench slip during the 2011 M_w 9.0 off the Pacific coast of Tohoku earthquake, *Earth Planets Space* **63,** 687–692, doi: 10.5047/eps.2011.05.033.

Mogi, K. (1969). Some features of recent seismic activity in and near Japan (2) Activity before and after great earthquakes, *Bull. Earthq. Res. Inst. Tokyo Univ.* **47,** 395–417.

Murotani, S., M. Kikuchi, Y. Yamanaka, and K. Shimazaki (2004). Rupture process of large Fukushima-Oki earthquakes (2), *Seismological Society of Japan (SSJ) Fall Meeting*, Hakozaki, Japan, P029.

Nakagawa, T, and Y. Oyanagi (1980). Program system SALS for nonlinear least squares fitting in experimental sciences, in K. Matusita (Editor), *Proceedings of Recent Developments in Statistical Inference and Data Analysis*, North Holland Publishing Company, Amsterdam, the Netherlands, 221–225.

Nettles, M., G. Ekström, and H. C. Koss (2011). Centroid-moment-tensor analysis of the 2011 off the Pacific coast of Tohoku earthquake and its

larger foreshocks and aftershocks, *Earth Planets Space* **63,** 519–523, doi: 10.5047/eps.2011.06.009.

Ohta, Y., R. Hino, D. Inazu, M. Ohzono, Y. Ito, M. Mishina, T. Iinuma, J. Nakajima, Y. Osada, K. Suzuki, H. Fujimoto, K. Tachibana, T. Demachi, and S. Miura (2012). Geodetic constraints on afterslip characteristics following the March 9, 2011, Sanriku-oki earthquake, Japan, *Geophys. Res. Lett.* **39,** L16304, doi: 10.1029/2012GL052430.

Okada, Y. (1992). Internal deformation due to shear and tensile faults in a half-space, *Bull. Seismol. Soc. Am.* **82,** 1018 – 1040.

Ozawa, S., T. Nishimura, H. Munekane, H. Suito, T. Kobayashi, M. Tobita, and T. Imakiire (2012). Preceding, coseismic, and postseismic slips of the 2011 Tohoku earthquake, Japan, *J. Geophys. Res.* **117,** no. B07404, 373–376, doi: 10.1029/2011JB009120.

Ozawa, S., T. Nishimura, H. Suito, T. Kobayashi, M. Tobita, and T. Imakiire (2011). Coseismic and postseismic slip of the 2011 magnitude-9 Tohoku-Oki earthquake, *Nature* **475,** 373–376, doi: 10.1038/nature10227.

Sato, T., S. Hiratsuka, and J. Mori (2012). Coulomb stress change for the normal-fault aftershocks triggered near the Japan Trench by the 2011 M_w 9.0 Tohoku-Oki earthquake, *Earth Planets Space* **64,** 1239 – 1243.

Sato, M., T. Ishikawa, N. Ujihara, S. Yoshida, M. Fujita, M. Mochizuki, and A. Asada (2011). Displacement above the hypocenter of the 2011 Tohoku-Oki earthquake, *Science* **332,** 1395, doi: 10.1126/science.1207401.

Shao, G., C. Ji, and D. Zhao (2011). Rupture process of the 9 March, 2011 M_w 7.4 Sanriku-Oki, Japan earthquake constrained by jointly inverting teleseismic waveforms, strong motion data and GPS observations, *Geophys. Res. Lett.* **38,** L00G20, doi: 10.1029/2011GL049164.

Shao, G., X. Li, C. Ji, and T. Maeda (2011). Focal mechanism and slip history of the 2011 M_w 9.1 Off the Pacific coast of Tohoku earthquake, constrained with teleseismic body and surface waves, *Earth Planets Space* **63,** 559–564, doi: 10.5047/eps.2011.06.028.

Suito, H., T. Nishimura, M. Tobita, T. Imakiire, and S. Ozawa (2011). Interplate fault slip along the Japan Trench before the occurrence of the 2011 off the Pacific coast of Tohoku earthquake as inferred from GPS data, *Earth Planets Space* **63,** 615–619, doi: 10.5047/eps.2011.06.053.

Suwa, Y., S. Miura, A. Hasegawa, T. Sato, and K. Tachibana (2006). Interplate coupling beneath NE Japan inferred from three-dimensional displacement field, *J. Geophys. Res.* **111,** no. B04402, doi: 10.1029/2004JB003203.

Takeuchi, M., T. Sato, and T. Shinbo (2008). Stress due to the interseismic back slip and its relation with the focal mechanisms of earthquakes occurring in the Kuril and northeastern Japan arcs, *Earth Planets Space* **60,** 549–557.

Tanaka, S. (2012). Tidal triggering of earthquakes prior to the 2011 Tohoku-Oki earthquake (M_w 9.1), *Geophys. Res. Lett.* **39,** L00G26, doi: 10.1029/2012GL051179.

Wessel, P., and W. H. F. Smith (1991). Free software helps map and display data, *Eos Trans. AGU* **72,** 441.

Yamamoto, Y., K. Obana, Y. Machida, K. Nakahigashi, M. Shinohara, K. Suzuki, Y. Ito, R. Hino, S. Kodaira, Y. Kaneda, Y. Murai, T. Sato, K. Uehira, H. Yakihara, K. Hirata, H. Tsushima, A. Yamazaki, H. Sugioka, A. Ito, and D. Suetsugu (2013). Structural heterogeneities around the shallow megathrust zone of the 2011 Tohoku earthquake, *Japan Geoscience Union Meeting*, Makuhari, Japan, 25 May 2013, SSS01–P02.

Yamanaka, Y., and M. Kikuchi (2004). Asperity map along the subduction zone in northeastern Japan inferred from regional seismic data, *J. Geophys. Res.* **109,** no. B07307, doi: 10.1029/2003JB002683.

Zhao, D., Z. Huang, N. Umino, A. Hasegawa, and H. Kanamori (2011). Structural heterogeneity in the megathrust zone and mechanism of the 2011 Tohoku-Oki earthquake (M_w 9.0), *Geophys. Res. Lett.* **38,** L17308, doi: 10.1029/2011GL048408.

Department of Earth and Environmental Sciences
Hirosaki University
Hirosaki 036-8162, Japan
tamao@cc.hirosaki-u.ac.jp
hiratsuka@mail.sci.hokudai.ac.jp
(T.S., S.H.)

Disaster Prevention Research Institute
Kyoto University
Kyoto 611-0011, Japan
mori@eqh.dpri.kyoto-u.ac.jp
(J.M.)

Manuscript received 13 February 2013;
Published Online 8 October 2013